1-2014

An empirically observed pitch-angle diffusion eigenmode in the Earth's electron belt near L* = 5.0

T. P. O'Brien
Aerospace Corporation

S. Claudepierre
Aerospace Corporation

J. B. Blake
Aerospace Corporation

Joseph F. Fennell
Aerospace Corporation

J. H. Clemmons
Aerospace Corporation

See next page for additional authors

Recommended Citation

O'Brien, T. P., S. G. Claudepierre, J. B.Blake, J. F. Fennell, J. H. Clemmons, J. L.Roeder, H. E. Spence, G. D. Reeves, andD. N. Baker (2014), An empirically ob-served pitch-angle diffusion eigenmodein the Earth's electron belt near L* = 5.0,Geophys. Res. Lett., 41, 251– 258,doi:10.1002/2013GL058713.

AGU PUBLICATIONS

Geophysical Research Letters

RESEARCH LETTER
10.1002/2013GL058713

Special Section:
Early Results From the Van Allen Probes

An empirically observed pitch-angle diffusion eigenmode in the Earth's electron belt near $L^* = 5.0$

T. P. O'Brien[1], S. G. Claudepierre[1], J. B. Blake[1], J. F. Fennell[1], J. H. Clemmons[1], J. L. Roeder[1], H. E. Spence[2], G. D. Reeves[3], and D. N. Baker[4]

[1]Space Sciences Department, The Aerospace Corporation, Los Angeles, California, USA, [2]Institute for the Study of Earth, Oceans, and Space, University of New Hampshire, Durham, New Hampshire, USA, [3]Space and Atmospheric Sciences Group, Los Alamos National Laboratory, Los Alamos, New Mexico, USA, [4]Laboratory for Atmospheric and Space Physics, University of Colorado Boulder, Boulder, Colorado, USA

Key Points:
- We observe a pure eigenmode of pitch angle diffusion in the radiation belt
- The eigenmode is characterized by synchronized decay at all pitch angles
- From the eigenmode, we derive a hypothetical pitch angle diffusion coefficient

Correspondence to:
T. P. O'Brien,
paul.obrien@aero.org

Citation:
O'Brien, T. P., S. G. Claudepierre, J. B. Blake, J. F. Fennell, J. H. Clemmons, J. L. Roeder, H. E. Spence, G. D. Reeves, and D. N. Baker (2014), An empirically observed pitch-angle diffusion eigenmode in the Earth's electron belt near $L^* = 5.0$, *Geophys. Res. Lett.*, *41*, 251–258, doi:10.1002/2013GL058713.

Received 14 NOV 2013
Accepted 7 JAN 2014
Accepted article online 8 JAN 2014
Published online 27 JAN 2014

Abstract Using data from NASA's Van Allen Probes, we have identified a synchronized exponential decay of electron flux in the outer zone, near $L^* = 5.0$. Exponential decays strongly indicate the presence of a pure eigenmode of a diffusion operator acting in the synchronized dimension(s). The decay has a time scale of about 4 days with no dependence on pitch angle. While flux at nearby energies and L^* is also decaying exponentially, the decay time varies in those dimensions. This suggests the primary decay mechanism is elastic pitch angle scattering, which itself depends on energy and L^*. We invert the shape of the observed eigenmode to obtain an approximate shape of the pitch angle diffusion coefficient and show excellent agreement with diffusion by plasmaspheric hiss. Our results suggest that empirically derived eigenmodes provide a powerful diagnostic of the dynamic processes behind exponential decays.

1. Introduction

The relativistic electrons in the Earth's outer radiation belt rarely, if ever, come to equilibrium. An equilibrium state would provide a straightforward, multidimensional probe into the dynamic processes that modify the quiescent radiation belts. However, the outer belt sometimes exhibits exponential decays lasting days, weeks, or even months [e.g., *Meredith et al.*, 2006; *Benck et al.*, 2010; *Su et al.*, 2012; *Fennell et al.*, 2013], and such decays are common in the inner zone [e.g., *Baker et al.*, 2007]. Exponentially decaying fluxes, when they are synchronized across one or more dimensions of the radiation belt phase space, indicate the presence of a pure eigenmode of a linear time evolution operator acting in one or more of the synchronized dimensions. This arises from the fact that the eigenvalue is a characteristic of the operator—if the eigenvalue changes along one or more dimension of the phase space—the operator must be changing along that dimension too.

In all likelihood, the relevant linear operator is a diffusion operator. The decay time is the negative reciprocal of the smallest eigenvalue, and the shape of the decaying eigenmode is a nearly unique transform of the diffusion coefficient. In practice, numerical uncertainty and the limitations of observations limit the derived diffusion coefficient to only part of the coordinate domain [*Schulz and Lanzerotti*, 1974, p 168]. Nonetheless, an eigenmode, which is a one- or higher-dimensional function, is necessarily a stronger constraint than the scalar decay time (eigenvalue) alone. The eigenmode can be synchronized in one, two, or three adiabatic invariants, depending on the order of the dominant diffusion process, although it is not necessarily possible to distinguish between multidimensional diffusion and lower order diffusion with a decay time that depends only weakly on one of the dimensions.

There is a fairly extensive literature on theoretical and empirical eigenmodes. The interested reader is directed to *Schulz and Lanzerotti* [1974], especially section V.2 which reviews the use of pitch angle eigenmodes. Also, *Albert and Shprits* [2009] update several of the Schulz and Lanzerotti calculations while describing the relationship among the shape of the longest-lived pitch angle diffusion eigenmode, the shape of the associated diffusion coefficient, and the decay time (eigenvalue).

Our analysis uses the drift invariants E (energy), K (Kaufmann's invariant) [*Kaufmann*, 1965], and L^* (Roederer's invariant) [*Roederer*, 1970]. The K and L^* invariants are also adiabatic invariants, while energy can be changed

by adiabatic processes such as storm time changes and secular changes in the Earth's magnetic field. However, E is invariant to reversible changes in the large-scale field geometry, thus making it resilient to storm time changes, once the transients have passed. We chose E because it minimizes the observational challenges associated with the true first invariant M (the relativistic magnetic moment): typical sensors measure particles as a function of energy, not M.

Using data from NASA's Van Allen Probes spacecraft, we have identified a case of synchronized decay of electron flux in the outer zone, near $L^* = 5.0$ during the interval 24 December 2012 to 12 January 2013. The decay has a time scale of about 4 days at ~593 keV. Flux at nearby energies and L^* values are also decaying exponentially, but, as we will see, only in the K (pitch angle) dimension is the decay time constant. We have deduced from this constant decay versus K that the primary mechanism is pitch angle scattering. Thus, this mechanism is likely associated with wave-particle interactions between the electrons and plasmaspheric hiss, which is present even under quiet conditions [*Thorne et al.*, 1973] (in the interval, the geomagnetic index Kp never exceeds 2+).

As we will see, radial and energy diffusion may very well be taking place, but at a low enough rate as to be negligible compared to the diffusion in pitch angle. We will use the shape of the flux versus K distribution to derive a hypothetical pitch angle diffusion coefficient. We show excellent agreement with the hiss hypothesis.

2. Instrumentation

The MagEIS (Magnetic Electron Ion Spectrometer) [*Blake et al.*, 2013] is part of the ECT (Energetic Particle, Composition, and Thermal Plasma) suite [*Spence et al.*, 2013] on NASA's Van Allen Probes (launched as Radiation Belt Storm Probes, RBSP). The electron portion of MagEIS consists of four magnetic spectrometers: a low (20–240 keV), medium (80–1200 keV), and high unit (800–4800 keV), plus a second medium unit tilted to provide additional local pitch angle coverage. There are two probes carrying this 4-sensor combination, and each probe spins at about 5.5 rpm allowing for rapid angle sampling. At ~600 keV, the MagEIS field of view is approximately 5° x 20°, with the larger dimension parallel to the vehicle's spin axis, which is roughly perpendicular to the magnetic field.

Each spectrometer employs a strong magnetic field to bend particles incident on the aperture through 180°, thereby creating an association between the energy and the location of the particle as it strikes the focal plane. The focal plane consists of solid-state detectors. Pulse height analysis of the energy deposits in the detectors allows for identification and removal of background. Throughout the mission and beyond, we expect the flux conversions and background subtraction for the MagEIS sensors to continually improve. For the purposes of our analysis, however, the absolute flux levels are not needed, only the relative intensity as a function of pitch angle, energy, and location.

3. Observations

The MagEIS fluxes are initially provided as a function of energy and spin angle sector. Each spin sector is assigned a local pitch angle using the onboard magnetometer [*Kletzing et al.*, 2013]. Since the energy channels evolve with sensor tuning, we have interpolated each sensor unit to a fixed set of energy channels. Using the satellite ephemeris and onboard magnetometry, we can assign magnetic coordinates to each MagEIS flux measurement. We compute daily fluxes in each energy channel on a set of bins in K and L^*, which are provided to us for the Tsyganenko 2004 (TS04) magnetic field model [*Tsyganenko and Sitnov*, 2005] by the ECT Science Operations Center (SOC) at Los Alamos National Lab. We compute the daily average flux in bins of K and L^* for each energy channel. The orbital period is about 9 h, giving approximately six passes through a given L^* range per day (three inbounds and three outbounds). We merge the two medium sensor units from the A vehicle to provide a combined, extended angular distribution over the medium energy range. By plotting the time series in any such bin, we have removed most (but not all) of the effects of large-scale magnetic field changes.

Figure 1a shows time evolution of several energy channels at $K = 61.5\ R_E\sqrt{\text{nT}}$ (equatorial pitch angle 43° in a dipole) and $L^* = 5.0$. From about 50 keV to about 3.5 MeV, there is a clear exponential decay from 24 December 2012 to 12 January 2013, marked by a thick horizontal bar. Particles with energies below 350 keV exhibit several injections. Particles above 1 MeV are also undergoing exponential decay during the marked interval, but clearly with a different decay time scale than those at ~593 keV, which are our focus. We have drawn (dashes) an exponential fit to the selected interval, and it is clear that several channels are decaying

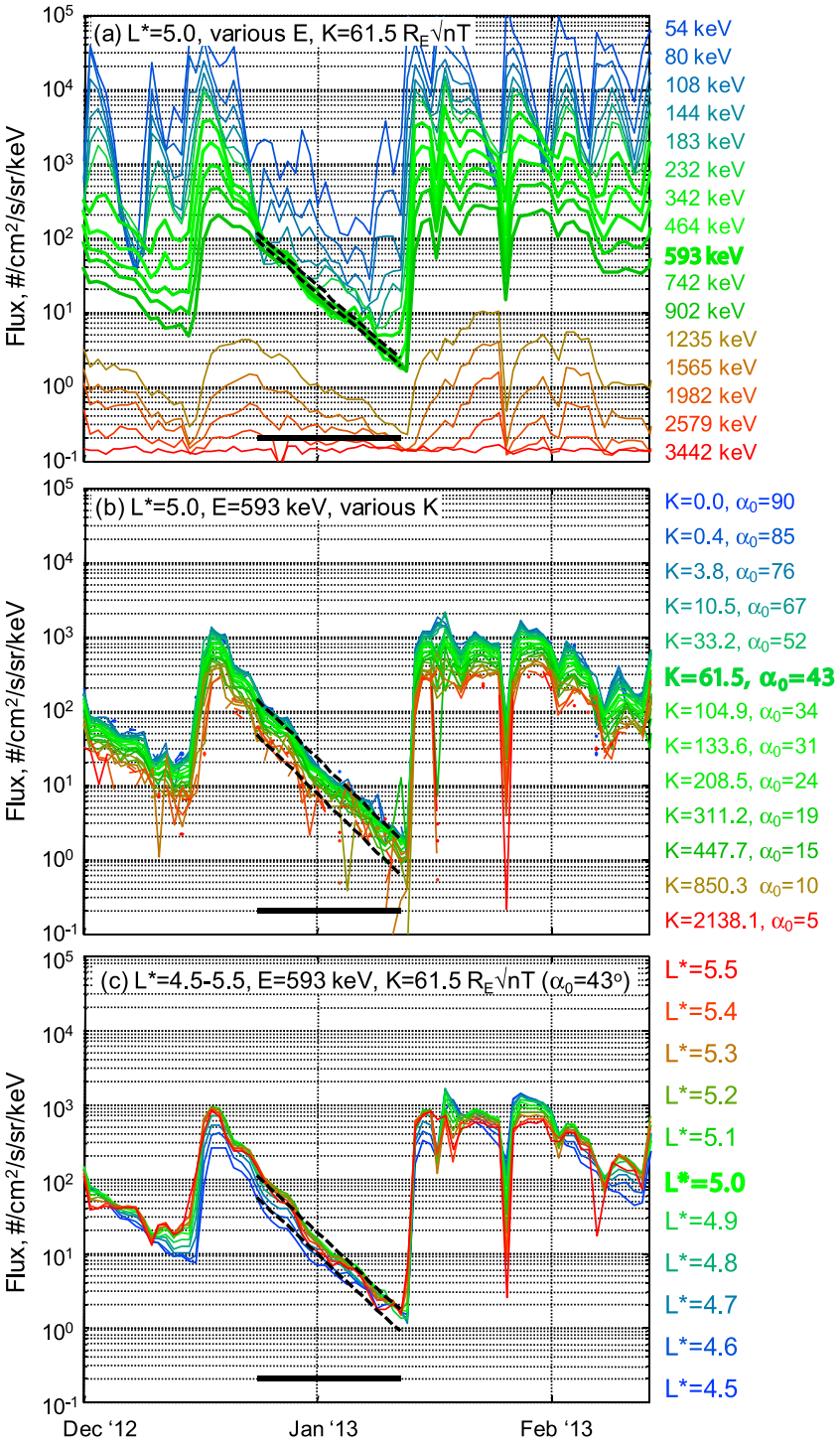

Figure 1. (a–c) The time series of daily averaged electron flux observed by the MagEIS instrument aboard Van Allen Probes at different energies, K, and L^* values in the outer zone. The horizontal black bar marks a period of observed exponential decay. The diagonal dashed lines outline the decay itself.

with a stable spectral shape and a decay time of about 4 days in agreement with *Meredith et al.* [2006]. Figure 1b shows time evolution of all the available K values at ~593 keV for $L^* = 5.0$ in the same format as Figure 1a. Again, there is a clear exponential decay in progress, and it involves all the observed Ks at the selected energy and L^*. Finally, Figure 1c shows the time evolution of fluxes at L^* ranging from 4.5 to 5.5 at

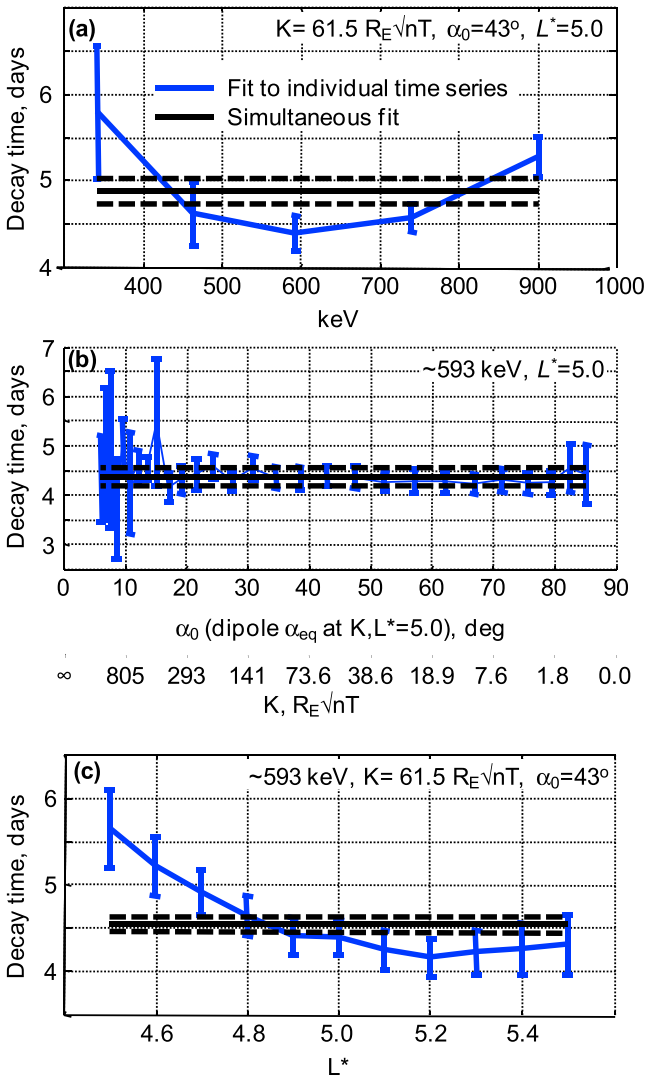

Figure 2. (a–c) The fitted decay times (blue) for corresponding traces from Figure 1. Error bars indicate 2 standard errors, or a 95% confidence interval. Black solid traces indicate a simultaneous fit to a single decay time along the plotted dimension, with a 95% confidence interval given by dashed lines.

~593 keV and $K = 61.5\ R_E\sqrt{nT}$. Although fluxes in the different L^* bins appear to be decaying at the same rate in Figure 1c, we shall show that they are actually decaying at different rates.

4. Analysis

Figure 1 reveals that there may be eigenmodes of E, K, and L^* diffusion present in the marked interval. To determine whether any of the observed exponential decays actually is an eigenmode, we must confirm that fluxes in different locations in phase space (different E, K, and L^*) are decaying with the same decay rate. To do that, we fit each trace to an exponential decay and compute the error on the determined decay time τ. Figure 2 shows the results of that fitting procedure—both fitting each trace individually to a decay time and fitting all traces in a given dimension simultaneously to a single decay time. The error bars indicate 2 standard deviations of the decay time (i.e., 2 standard errors) and thus approximate a 95% confidence interval. It is clear that only for the K dimension are the decays consistent with a single decay time across the entire dimension. *Su et al.* [2012] also concluded there was no dependence on pitch angle, while multiple studies have found a dependence on energy and L^* [*Meredith et al.*, 2006; *Baker et al.*, 2007; *Benck et al.*, 2010; *Su et al.*, 2012; *Fennell et al.*, 2013]. Thus, we conclude that we are observing an eigenmode of *only* (i.e., elastic) pitch angle diffusion at ~593 keV and $L^* = 5.0$, with other processes being negligible, locally. In particular, we are probably observing the longest-lived

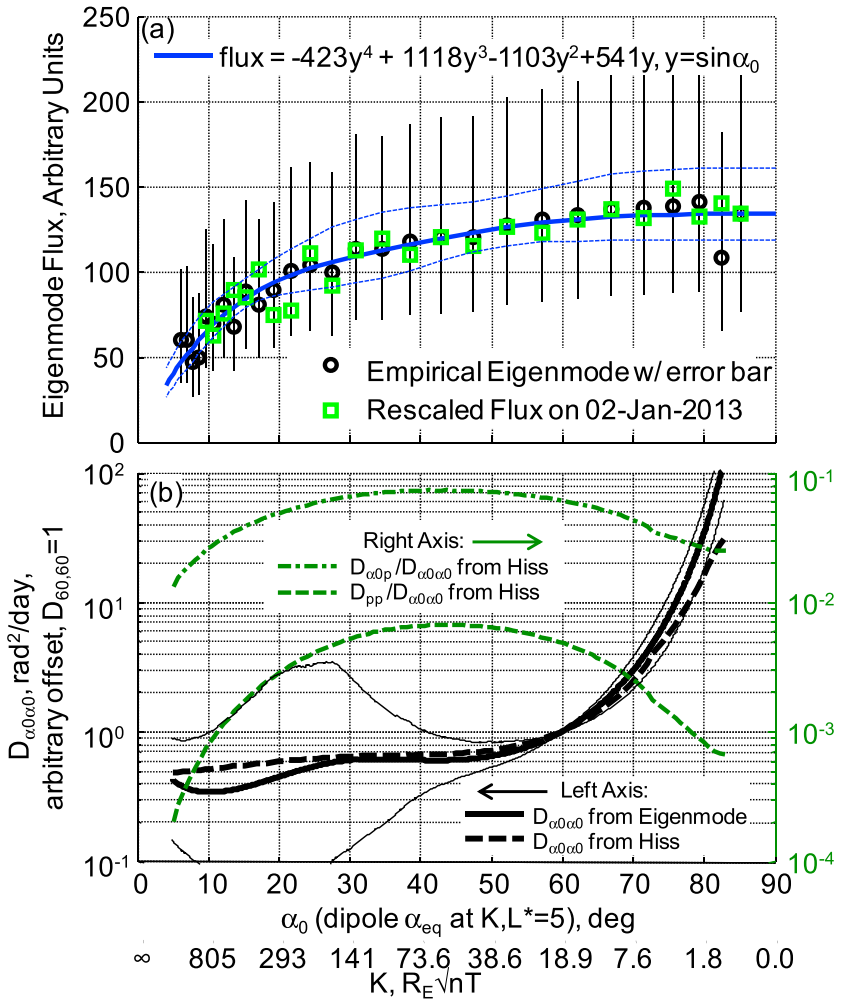

Figure 3. (a) The empirical eigenmode (black) and 95% confidence, obtained by fitting all *K* values at L^* = 5.0 and ~593 keV over the interval marked in Figure 1. Green squares indicate the (rescaled) flux on 2 January 2013 as an example, and the blue curve provides a polynomial fit of the eigenmode shape, with a 95% confidence marked in thin blue dashed lines. (b) The pitch angle diffusion coefficient derived from the polynomial shape for the eigenmode (solid black, left axis) and that from hiss (dashed black, left axis). The diffusion coefficient has an arbitrary offset and is depicted here with a diffusion coefficient of unity at 60° and a 95% confidence interval (thin black lines). Also shown are the ratios of the other two diffusion coefficients for hiss (green curves, right axis) relative to pitch angle diffusion. Note: the abscissa is given in degrees, while the ordinate is in rad^2/d.

eigenmode, as one would expect other injections and other magnetospheric processes to stimulate all eigenmodes, and the time series only becomes exponential after the shorter-lived modes have decayed away.

Figure 3a gives the eigenmode shape at ~593 keV based on the simultaneous fit of all the *K* values to a single decay time with a different flux scale factor for each *K* bin. We also show the *K* distribution for an example day. For comparison to the conventional depiction of angular distributions and diffusion coefficients, we convert from *K* in the TS04 field to the corresponding equatorial pitch angle (α_{eq}) in a dipole at L^* = 5.0, which we denote α_0. The transform between *K* and α_0 is given by

$$K = Y(y)L^*\sqrt{B_m} \quad (1)$$

where *Y(y)* is a function of field line topology, *y* is the sine of the counterpart dipole equatorial pitch angle, and B_m is the mirror magnetic field strength [*Schulz and Lanzerotti*, 1974]. As in Figure 2, the error bars in Figure 3a indicate 2 standard deviations, or approximately a 95% confidence interval. The black error bars indicate the error in the flux scale factor of the exponential decay fit versus time for each *K* bin. The blue dashed error bars indicate the error in the polynomial fitting of those flux factors versus α_0. We have fit the

eigenmode shape to a polynomial in y, with the constraint that the slope of the fit is zero at 90° and the polynomial is zero at 0° (these are consistent with our boundary conditions below).

Continuing with the dipole approximation, we examine the 1-D diffusion equation for pitch angle diffusion at constant energy and L^* [from *Schulz and Lanzerotti*, 1974, pp 77]:

$$\frac{\partial f}{\partial t} = \frac{1}{xT(y)} \frac{\partial}{\partial x} \left[xT(y) D_{xx} \frac{\partial f}{\partial x} \right] \tag{2}$$

where f is the phase space density (proportional to flux when diffusing at constant energy), x is the cosine of α_{eq}, D_{xx} is the diffusion coefficient (which also depends on x), and $T(y)$ is a field line geometry factor. For a dipole, $T(y)$ is approximated by [*Schulz and Lanzerotti*, 1974, pp 19]

$$T(y) = 1.3802 - 0.3198(y + \sqrt{y}) \tag{3}$$

The boundary conditions are

$$\left. \frac{\partial f}{\partial x} \right|_{x=0} = 0 \tag{4}$$

$$f(1) = 0 \tag{5}$$

The first boundary condition represents symmetry about 90° equatorial pitch angle, which is a consequence of bounce phase mixing, and the second represents the loss cone (which is technically at x somewhat less than 1).

In representing the diffusion in terms of dipole coordinates, we are effectively assuming that the field line geometry, averaged over the $L^* = 5.0$ drift shell, is approximately a dipole in the quiet interval we have selected for study. *Orlova and Shprits* [2010] have shown that in a quiet field, the nondipole field has little impact on the diffusion coefficient even at local midnight where the field is most nondipolar, and so, our approximation should hold true.

For a pure eigenmode v of pitch angle diffusion, with eigenvalue $-1/\tau$, we have

$$\frac{\partial v}{\partial t} = -\frac{v}{\tau} = \frac{1}{xT(y)} \frac{\partial}{\partial x} \left[xT(y) D_{xx} \frac{\partial v}{\partial x} \right] \tag{6}$$

We can invert this expression to obtain D_{xx} relative to a reference value D_0 (i.e., D_{xx} at $x_0 = 0.5$):

$$D_{xx} = \frac{1}{xT(y)\frac{\partial v}{\partial x}} \left[x_0 T(x_0) \left. \frac{\partial v}{\partial x} \right|_{x_0} D_0 - \int_{x_0}^{x} \frac{v}{\tau} xT(y) \mathrm{d}x \right] \tag{7}$$

We note that the expression includes $x\frac{\partial v}{\partial x}$ in the denominator, which means it may diverge near $x = 0$ (90°) because both x and $\frac{\partial v}{\partial x}$ are zero at $x = 0$. In fact, our empirical eigenmode is flat for pitch angles 60–90°, suggesting a very large diffusion coefficient for $x < 0.5$ or $\alpha_0 > 60$.

Figure 3b shows the inverted diffusion coefficient for ~593 keV electrons at $L^* = 5.0$ during this event. The vertical position in the plot is arbitrary, as we have forced the diffusion coefficient to unity at 60° (Note: $D_{\alpha_0\alpha_0} = D_{xx}/y^2$, and we represent it in rad^2/d). What we see is that the steepest positive gradient in the eigenmode occurs below 30° and corresponds to a region of relatively small diffusion coefficient. (The uncertainty is large near 30° because of the uncertain location of the gradient in the eigenmode.) The weak diffusion near the low pitch angle steepening of the eigenmode is consistent with the idea that diffusion smoothes out gradients, and so, a long-lived slope must be the result of locally weak diffusion. Also shown in Figure 3b is an estimate of $D_{\alpha_0\alpha_0}$ from plasmaspheric hiss. The wave amplitude and azimuth weighting are lost in the normalization at 60°, while the wave properties are taken from *Meredith et al.* [2006]: a Gaussian centered at 0.55 kHz, with a standard deviation of 0.3 kHz, a lower bound of 0.1 kHz, and an upper bound of 2 kHz. We limit the hiss to magnetic latitudes below 45° [*Shprits et al.*, 2011]. We use the plasmaspheric density values from *Sheeley et al.* [2001]. We compute the diffusion coefficients using the field-aligned assumption of *Summers* [2005], and we perform the bounce averaging in a dipole, using the method of *Orlova and Shprits* [2011]. We note that *Meredith et al.* [2006] and *Orlova and Shprits* [2011] explored the field-aligned and dipole assumptions and found them suitable for quiet times. The agreement between the eigenmode-derived shape of $D_{\alpha_0\alpha_0}$ agrees well with that derived from the assumed hiss interaction. Further, diffusion in momentum p and cross

diffusion in angle and momentum (green traces in Figure 3b) associated with hiss are negligible by at least a factor of 10 relative to pitch angle diffusion.

While the eigenmode analysis can only specify the diffusion coefficient to within a constant *additive* offset (D_0 in 7), our plasmaspheric hiss diffusion coefficient is *multiplicatively* rescaled to give $D_{\alpha_0\alpha_0} = 1$ rad^2/d at 60°. The excellent agreement in the shape of the two diffusion coefficients away from 60° in Figure 3b suggests that the choice of $D_{\alpha_0\alpha_0}$ is fortuitous. Attempts to actually tune the parameters of the wave model to an observed eigenmode should select D_0 from the wave model, rather than setting it a priori to the convenient value of 1 rad^2/d as we have done.

5. Discussion and Conclusion

We have presented observations of several exponentially decaying flux time series in the outer zone near $L^* = 5.0$. A detailed examination shows that the decay times depend on energy and L^* but not on K. Therefore, we conclude that the exponential decay is a pure eigenmode of elastic pitch angle (K) diffusion (i.e., at constant energy). We empirically estimate the shape and decay value of the eigenmode and, from those, estimate the associated equatorial pitch angle diffusion coefficient. We show that the diffusion coefficient is relatively small for angles below 60° equatorial pitch angle, corresponding to a steepening of the gradient in the eigenmode. We also show that the specific diffusion process (elastic angle scattering) and the shape of the diffusion coefficient are consistent with plasmaspheric hiss. We note that the eigenmode analysis fundamentally includes drift averaging, which cannot be done easily using in situ wave data alone because of the need to cover the complete drift orbit with a sparse constellation of satellites.

A preliminary inspection of high-frequency receiver data from the Electric and Magnetic Field Instrument Suite and Integrated Science (EMFISIS) on Van Allen Probes [*Kletzing et al*., 2013] suggests that $L^* = 5$ is inside the plasmasphere for much of the interval (C. Kletzing, private communication, 2013). According to the Electric Field and Waves (EFW) experiment [*Wygant et al*., 2013], the plasmapause is beyond $L^* = 5.0$ for much of the study interval, and hiss waves are present inside the plasmasphere (A. N. Jaynes et al., Evolution of relativistic outer belt electrons during extended quiescent period, submitted to *Geophys. Res. Lett*., 2013).

We have investigated (not shown) whether the eigenmode or diffusion coefficient depends on energy from 300 to 900 keV and L^* from 4.5 to 5.5. We have not found any significant variation, within the limits of the data. Thus, the essential property of what we report is a broad flat top in the eigenmode from 60–90° equatorial pitch angle. This indicates much stronger pitch angle diffusion in that range of angles, versus 0–60°, where the steeper gradient indicates weaker diffusion. We expect that this feature can be used as a constraint on the wave and plasma properties assumed in quasilinear diffusion calculations. In particular, it is consistent with strong resonance with hiss occurring only for equatorial pitch angles above 60°.

We note that our choice of E, K, L^* coordinates was somewhat fortuitous. If elastic pitch angle diffusion is dominant, then it would be somewhat obscured in an analysis that used the canonical first two invariants J_1 and J_2, which both depend on particle energy [*Schulz and Lanzerotti*, 1974, pp. 11–12], or M and K because angle scattering alters M at constant E. In either a J_1,J_2 or a M,K system, it would still be possible to discover that decay time is invariant to energy. For example, a contour plot of decay time versus J_1 and J_2 would reveal a set of trajectories along which decay time is constant, and one could deduce that such trajectories corresponded to constant energy contours in the J_1, J_2 plane. Further, if one examined the decay time as a function of all three invariants, there would almost certainly be two-dimensional surfaces of constant decay time. These isosurfaces could, in principle, indicate two-dimensional diffusion in some tailored coordinate system [c.f., *Albert and Young*, 2005]; alternatively, they could simply represent one-dimensional diffusion with a decay time that is invariant (at least locally) to one other phase-space coordinate. To distinguish these two interpretations would require examination of the shape of the isosurfaces as well as interrogation of hypothetical diffusion mechanisms for consistency with the implied tailored coordinate system. Such an analysis is beyond the scope of the present investigation.

Acknowledgments
The authors acknowledge useful discussions with M. Schulz, Y. Shprits, J. Albert, and our colleagues at The Aerospace Corporation. The authors acknowledge H. Funsten for contributions to the ECT suite and C. Kletzing for examining the EMFISIS data. The magnetic coordinates for the Van Allen Probes vehicle were provided by the ECT SOC at Los Alamos National Lab. We obtained the *Kp* magnetic activity index from the OMNI data set. The OMNI data were obtained from the GSFC/SPDF OMNIWeb interface at http://omniweb.gsfc.nasa.gov. This work was funded by contract 10-068 from the University of New Hampshire, derived from NASA Van Allen Probes mission funding via RBSP-ECT funding NAS5-01072 provided by JHU/APL contract 967399.

The Editor thanks one anonymous reviewer for his/her assistance in evaluating this paper.

References

Albert, J. M., and S. L. Young (2005), Multidimensional quasi-linear diffusion of radiation belt electrons, *Geophys. Res. Lett.*, *32*, L14110, doi:10.1029/2005GL023191.

Albert, J. M., and Y. Y. Shprits (2009), Estimates of lifetimes against pitch angle diffusion, *J. Atmos. Sol. Terr. Phys.*, *71*, 1647–1652, doi:10.1016/j.jastp.2008.07.004.

Baker, D. N., S. G. Kanekal, R. B. Horne, N. P. Meredith, and S. A. Glauert (2007), Low-altitude measurements of 206 MeV electron trapping lifetimes at $1.5 \leq L \leq 2.5$, *Geophys. Res. Lett.*, *34*, L20110, doi:10.1029/2007GL031007.

Benck, S. L., M. Mazzino, J. C. Cyamukungu, and V. Pierrard (2010), Low altitude energetic electron lifetimes after enhanced magnetic activity as deduced from SAC-C and DEMETER data, *Ann. Geophys.*, *28*, 849–859.

Blake, J. B., et al. (2013), The Magnetic Electron Ion Spectrometer (MagEIS) instruments aboard the Radiation Belt Storm Probes (RBSP) spacecraft, *Space Sci. Rev.*, *179*, 383–421, doi:10.1007/s11214-013-9991-8.

Fennell, J.F., Blake, J.B., Friedel, R., and Kanekal, S. (2013) The energetic electron response to magnetic storms: HEO satellite observations, in *The Inner Magnetosphere: Physics and Modeling*, edited by T. I. Pulkkinen, N. A. Tsyganenko, and R. H.W. Friedel, AGU, Washington, D. C., doi:10.1029/155GM10.

Kaufmann, R. L. (1965), Conservation of the first and second adiabatic invariants, *J. Geophys. Res.*, *70*, 2181–2186.

Kletzing, C. A., et al. (2013), The Electric and Magnetic Field Instrument Suite and Integrated Science (EMFISIS) on RBSP, *Space Sci. Rev.*, *179*, 127–181, doi:10.1007/s11214-013-9993-6.

Meredith, N. P., R. B. Horne, S. A. Glauert, R. M. Thorne, D. Summers, J. M. Albert, and R. R. Anderson (2006), Energetic outer zone electron loss timescales during low geomagnetic activity, *J. Geophys. Res.*, *111*, A05212, doi:10.1029/2005JA011516.

Orlova, K. G., and Y. Y. Shprits (2010), Dependence of pitch-angle scattering rates and loss timescales on the magnetic field model, *Geophys. Res. Lett.*, *37*, L05105, doi:10.1029/2009GL041639.

Orlova, K. G., and Y. Y. Shprits (2011), On the bounce-averaging of scattering rates and the calculation of bounce period, *Phys. Plasmas*, *18*, 092904, doi:10.1063/1.3638137.

Roederer, J. G. (1970), *Dynamics of Geomagnetically Trapped Radiation*, Springer-Verlag, New York.

Schulz, M., and L. J. Lanzerotti (1974), *Physics and Chemistry in Space, Particle Diffusion in the Radiation Belts*, vol. 7, Springer, New York.

Sheeley, B. W., M. B. Moldwin, H. K. Rassoul, and R. R. Anderson (2001), An empirical plasmasphere and trough density model: CRRES observations, *J. Geophys. Res.*, *106*, 25,631–25,641.

Shprits, Y., D. Subbotin, B. Ni, R. Horne, D. Baker, and P. Cruce (2011), Profound change of the near-Earth radiation environment caused by solar superstorms, *Space Weather*, *9*, S08007, doi:10.1029/2011SW000662.

Spence, H. E., et al. (2013), Science goals and overview of the Radiation Belt Storm Probes (RBSP) Energetic Particle, Composition, and Thermal Plasma (ECT) suite on NASA's Van Allen Probes mission, *Space Sci. Rev.*, *179*, 311–336, doi:10.1007/s11214-013-0007-5.

Su, Y.-J., W. R. Johnston, J. M. Albert, G. P. Ginet, M. J. Starks, and C. J. Roth (2012), SCATHA measurements of electron decay times at $5 < L \leq 8$, *J. Geophys. Res.*, *117*, A08212, doi:10.1029/2012JA017685.

Summers, D. (2005), Quasi-linear diffusion coefficients for field-aligned electromagnetic waves with applications to the magnetosphere, *J. Geophys. Res.*, *110*, A08213, doi:10.1029/2005JA011159.

Thorne, R. M., E. J. Smith, R. K. Burton, and R. E. Holzer (1973), Plasmaspheric hiss, *J. Geophys. Res.*, *78*, 1581–1596.

Tsyganenko, N. A., and M. I. Sitnov (2005), Modeling the dynamics of the inner magnetosphere during strong geomagnetic storms, *J. Geophys. Res.*, *110*, A03208, doi:10.1029/2004JA010798.

Wygant, J. R., et al. (2013), The Electric Field and Waves instruments on the Radiation Belt Storm Probes, *Space Sci. Rev.*, *179*, doi:10.1007/s11214-013-0013-7.